# Portable Exoskeleton Glove with Soft Structure for Hand Assistance in Activities of Daily Living

Dmitry Popov, Igor Gaponov, *Member, IEEE,* and Jee-Hwan Ryu, *Member, IEEE*

***Abstract*—This paper presents a new portable exoskeleton glove developed for assistance in activities of daily living (ADL). The proposed glove is soft, adjustable, allows unconstrained motion of the wrist and leaves the palm free for object grasping and manipulation. In the proposed design, both flexion and extension motions of the thumb and three fingers (excluding the little finger) are supported by respective bidirectional actuators. The kinematics of the device were derived and are presented along with an experimental evaluation. The developed glove system is compact and light, with the weights of the wearable part and the whole system being 250 g and 340 g, respectively. The maximum pinch force provided by the device was experimentally measured to be 16 N, which gives the proposed device one of the highest power-to-weight ratio among existing portable devices for hand ADL assistance. The usability of the developed device was verified in a series of indoor and outdoor tests. The glove allowed test subjects to hold and manipulate versatile objects with diameters up to 90 mm and weighing 300 g. When powered by a conventional 3000-mAh battery, the glove could operate continuously performing grasping task for 4 hours.**

***Index Terms*—Cable-driven glove, exoskeleton, wearable robot.**

## I. Introduction

THE human hand is one of the most important systems we have for interacting with the environment, as it provides sensory and haptic feedback, as well as the ability to manipulate objects. Studies have shown that, on average, a person performs 1500 grasps with the hand per day [1]. However, there are millions of people worldwide suffering from hand function impairment, and this number is constantly growing. Hand functioning and coordination may be compromised by various causes, the most common of which include traumas and injuries such as spinal cord injury, degenerative diseases, stroke, various motor disabilities and muscle weakness associated with aging. For example, the studies suggest that in stroke survivors, hand is the most likely limb to be affected [2], [3]. If one's hand function is compromised, it may significantly limit the number of daily tasks that the person can perform and result in a lower quality of life [4]. For this reason, therapists and doctors have been developing various approaches and methods to restore normal functionality to impaired parts of the body.

The most common approach to improve the hand functionality is rehabilitation through physical therapy. However, the number of people with hand impairment in modern society is constantly growing, partly because of the growth in older population. As a result, it is not always possible to provide every patient with a sufficient level of therapist' involvement. Additionally, the large number of repetitive exercises involved in each therapy session makes the job of doctors monotonous and does not fully exploit their qualifications and experience.

To decrease the burden on specialists, engineers have developed various robotic devices to automate the therapy. These devices do not only ease the therapists' workload, but also help to improve therapy conditions for the patients. Experimental studies have confirmed that the use of robotic systems for post-stroke and post-trauma physical therapy under doctors' supervision improves motor functions of the patients [5], [6].

A number of hand rehabilitation systems have been developed to date. For instance, Ueki et al. developed and experimentally evaluated an 18-DOF hand rehabilitation robot for virtual reality-enhanced therapy [7]. Moromugi et al. designed a tendon-driven glove for hand assistance [8]. Hyunki In et al. developed a soft tendon-driven system to assist grasping motion for people with spinal cord injuries [9]. A commercially available system, Gloreha 2 Pro, provides virtual reality-enhanced rehabilitation for stroke patients [10]. For a more comprehensive overview of existing upper-limb rehabilitation devices, including exoskeleton gloves, the reader is referred to a detailed survey on the topic [11].

However, devices that are presently used for rehabilitation are mainly restricted to use in a hospital environment because of their large size and weight, high cost, and low mobility. At the same time, rehabilitation as an approach does not guarantee full recovery of the motor-sensory functions of the affected limb, and therefore patients often do not have the functionality of their hands restored completely after the therapy. Some studies have shown that approximately 70% to 80% of stroke survivors require long-term medical care [17], while at least 50% of the patients have to live with chronic impairments [2]. This results in poor quality of life for the patients, who are often left needing assistance to perform the activities of daily living (ADL).

The statistics mentioned above highlight the importance of, and demand for, robotic systems that can assist people who have disabilities in performing the activities of daily living on a regular basis. However, developing an active device suitable for hand assistance in ADL is a challenging task,

D. Popov, I. Gaponov and J.-H. Ryu are with the School of Mechanical Engineering, Korea University of Technology and Education, 1600 Chungjeolno, Cheonan, Chungnam, 31253 South Korea e-mail: {dmitry,igor,jhryu}@koreatech.ac.kr

This research was supported by National Research Foundation of Korea (NRF) grant funded by the Korean government (MSIP)(No. NRF-2013R1A2A1A03069658) and the grant "Development of core teleoperation technologies for maintaining and repairing tasks in nuclear power plants" funded by the Ministry of Trade, Industry and Energy of S. Korea

Manuscript received November 25, 2015; revised July 23, 2015.

This article has been accepted for publication in a future issue of this journal, but has not been fully edited. Content may change prior to final publication. Citation information: DOI 10.1109/TMECH.2016.2641932, IEEE/ASME Transactions on Mechatronics



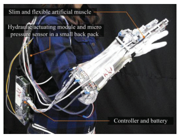
Ryu et al., 2008 [12]

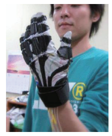
Moromugi et al., 2009 [8]

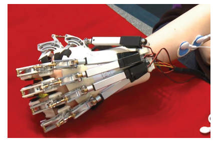
Hand of Hope, 2013 [13]

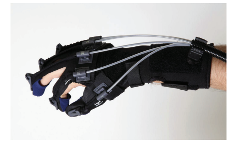
Gloreha 2, 2013 [14]

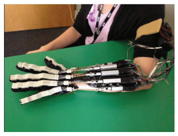
X-Glove, 2014 [15]

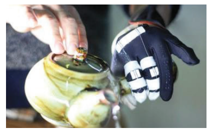
SNU Exo-Glove, 2015 [9]

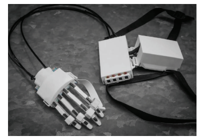
Nycz et al., 2016 [16]


GraspyGlove (this paper), 2016

Fig. 1. Some of the existing wearable hand-assistance and rehabilitation robotic systems

since the robotic system should be portable and fully wearable, allowing the person to move around freely, as if there was no external system helping her or him. This requirement makes it important for such devices to have a high power-to-weight ratio. Additionally, the system should be able to support a wide range of hand synergies, assist in both hand flexion and extension and should not interfere with the natural movements of other joints of the arm, such as the wrist.

Diverse approaches have been previously utilized to develop systems for hand assistance and rehabilitation, where each of the approaches satisfied one or several requirements mentioned above, and some of the exoskeleton devices are shown in Fig. 1. Of the portable hand support systems, Ryu et al. developed a haptic glove powered by a miniaturized hydraulic system and artificial muscles [12]. However, the original version of the device was comparatively heavy (2.74 kg). Triandafilou et al. experimentally evaluated a 5-DOF device named X-Glove in a series of cyclical stretch experiments on patients with subacute stroke [15], however, very few details and characteristics of this device are reported. Tong et al. developed a commercially available 5-DOF EMG-based wearable exoskeleton named 'Hand of Hope' for post-stroke hand physical therapy [13]. However, the rigid links and joints of the device require accurate alignment with finger joints, making the device relatively bulky at the same time. Nycz et al. developed a cable-driven glove with an integrated EMG measurement system for hand rehabilitation [16]. This system is highly portable, with the weight of the wearable part being as low as 113 g. However, the device did not provide thumb actuation, while the rest of the four fingers were actuated together. In addition, the glove had a relatively low efficiency due to energy losses in the Bowden cable transmission. Diftler et al. have presented the RoboGlove system, which can be used for human power amplification [18]. The device weighed approximately 770 g, could generate up to 90 N power grasping force and may be potentially used in rehabilitation. However, the main application of this device is currently power assistance for industrial workers, and it is not clear if the device can be used for ADL assistance in its present state, as only the grasping motion is supported. To the best of our knowledge, there are currently no available devices that assist hand synergies in ADL, with the limited portability, small output force or increased weight being the main flaws of the existing systems.

This paper proposes a fully portable and wearable hand assistive system designed to support ADL. The developed device is a glove-type exoskeleton that actuates three fingers (excluding the little finger) and a thumb. The proposed glove supports both flexion and extension. In addition, it allows for free motion of the wrist and has one of the highest output power-to-weight ratio among existing portable glove systems [12]-[15]. The maximum pinch force was experimentally measured to be 16 N, while the weight of the whole system is 340 g. The glove is capable of performing both a precision grip and a power grip.

The main contribution of this paper is the proposal of a new design concept for a hand assistive device that is capable of supporting ADL, by having sufficient power while maintaining portability. Although there are other existing systems that employ similar design principles, to the best of our knowledge, none of them can satisfy the requirements of portability and high power-to-weight ratio simultaneously. In the proposed glove design, instead of rigid links and joints a soft structure was implemented, which allows the device to be compact. Employing a single motor which supports both flexion and extension per finger, leads to a lighter glove. Lastly, the motors are placed directly on the dorsal side of the hand, which improves transmission efficiency. All these features together make the overall system portable while maintaining a high power-to-weight ratio. Additional details on the performance and design features of the proposed exoskeleton glove are presented in the following sections.

It should be specifically noted that this paper is not concerned with development of a particular algorithm or hardware to detect human intention, since this will vary depending on the target patient group [19]. The device described in this paper only employs basic triggering tools and algorithms (manual control and automatic object grasp), which are necessary for the evaluation of the performance of the developed glove. We believe that the proposed device in its current form can be used to assist patients of various target groups, and we are planning to develop specific control and triggering algorithms for specific target groups as a part of our future research.

This article has been accepted for publication in a future issue of this journal, but has not been fully edited. Content may change prior to final publication. Citation information: DOI 10.1109/TMECH.2016.2641932, IEEE/ASME Transactions on Mechatronics



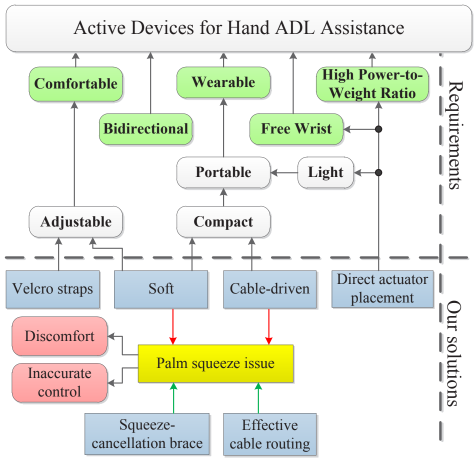


Fig. 2. General requirements for devices for hand assistance in ADL and our solutions

## II. Requirements and Challenges for Hand Assistive System

This section describes major requirements for the devices intended for hand assistance in ADL. We could not find a similar list of the most essential characteristics reported elsewhere. However, as a result of the analysis of available literature [11] and consultations with rehabilitation specialists and doctors, we could summarize the main requirements for hand assistance devices as follows:

- Bidirectionality: The system should preferably support both finger flexion and extension and be capable of controlling each finger separately.
- Wearability: The device should be wearable (which implies complete portability) so that the user can move around freely while wearing the device.
- High Power-to-Weight Ratio: The system should be light and compact while capable of generating sufficient output force and velocity, which implies an exoskeleton with a high power-to-weight ratio.
- Free wrist and palm: The device should allow object grasping and should not impose any constraints on the mobility of other joints of the arm, such as the wrist.
- Safety and comfort: The device must be safe and comfortable for the wearer.

These requirements are summarized graphically in Fig. 2. It is challenging to satisfy all of the requirements in one exoskeleton system, with the major hurdles being limited space, trade-off between positioning accuracy and compactness and weight, and the need of efficient and easy-to-maintain actuators.

Firstly, the human hand has a high number of degrees of freedom and a significantly limited space for hardware installation. Therefore, actuators should either be installed remotely from the hand or be very compact and light in the case of direct installation on the palm. Both of these cases are challenging, since remote actuation requires an efficient force transmission mechanism, while compact actuators might not produce sufficient power.

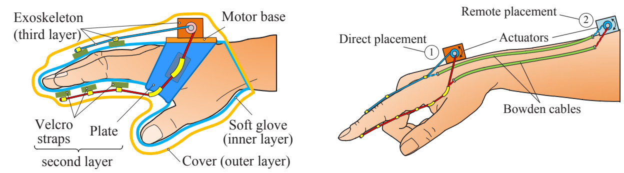


Fig. 3. Side view of the GraspyGlove (left); Possible actuators' locations

Secondly, the need for a light device calls for the use of either a light-weight rigid or a soft frame. However, having rigid mechanical links is undesirable because they need to be well-aligned with human joints and often lead to a bulky structure. On the other hand, having a soft frame may introduce undesirable deformations of the frame and cause additional parasitic motions.

Lastly, selecting suitable actuators and transmission mechanisms is another challenging issue. Hydraulic and pneumatic actuators are often used in robotic systems due to their high power density and easy power transmission. However, they are demanding in terms of maintenance, since one needs to prevent air or oil leakages, water ingress, oxidation, and other undesirable factors. Conversely, conventional electric motors, in combination with mechanical gears and power transmission systems, can be quieter, cheaper, more durable and require less maintenance. In addition, electric batteries which can power the motors are generally more compact than pressure pumps used by pneumatic and hydraulic actuators. However, mechanical transmission mechanisms (gears, belts, Bowden cables) that are required to transfer power from the motors to the end-effector often suffer from low efficiency, mechanical complexity, alignment issues, and other problems.

All of these challenges need to be addressed to design an assistive device suitable for ADL applications.

## III. Glove Design

### A. Structure of the Glove

This section provides the details on design of the proposed exoskeleton glove. The developed device may consist of 2 to 4 layers, as shown in Fig. 3, left:

- The inner layer, which can be any soft glove worn to increase the wearer's comfort.
- The second layer is made of stiff material (e.g. leather or hard rubber, Velcro straps), onto which the actuators and cable guides can be mounted. It also includes a rigid plate which repeats the anatomical shape of the hand and prevents undesired lateral deformations of the glove during operation.
- The third layer is the actual exoskeleton system (actuators and cables) which drives the fingers.
- The fourth (outermost) layer can be used to cover the actuators and cables of the exoskeleton (*optional*).

All these layers are then assembled into a single device, so that the user does not need to wear them separately. The motor base is attached to the inner layer of the glove on the dorsal side of the palm. The actuators are rigidly mounted onto the base to prevent their slippage during actuation. Elastic cables made of a low-friction material pass through the guides attached on the front (palmar) and back (dorsal) sides of the fingers. Each pair of front and back cables is connected to a respective capstan of the actuator (a geared DC motor). These capstans consist of two interconnected cylinders. When the motor starts to rotate, one tendon wraps around the pulley while the other one unwinds from it, which results in the flexion or extension of the finger.

The kinematics of the dorsal and palmar cables is different and therefore it should be taken into account so that the motors do not produce slack or cause interference between the cables during operation. We have investigated several ways to solve the tensioning issue, with one of them being a conventional spring-based tensioner mechanism placed on the dorsal side of the palm. However, such mechanism occupied substantial space and introduced mechanical complexity into the glove design, and therefore we had to search for other solutions. Our final approach was to take into account the difference in tendon kinematics and to design the motor capstans accordingly, with different capstan diameters for each cable. Although this design involved customization process it did not need much installation space and simplified the mechanical structure of the glove significantly. This design could have produced minimal amount of slack in some grasping scenarios due to the compliance of the glove. However, we have used an inextensible glove which was tightly fit to the wearer's hand in order to minimize the compliance of the device. As a result, the magnitude of the slack was normally on the order of several millimeters and did not severely affect the performance of the glove. To prevent the cables unwinding from the motors, we installed mechanical caps around each capstan. We employed the following procedure to initially adjust the cable tension: Firstly, only the flexor cables were installed at each actuator and contracted to fully flex the fingers. Next, the extensor cables were connected, and their length was adjusted to prevent any slack. As a result, the cables could be driven by the pulleys of different diameters in accordance with finger kinematics, and thus the slack was prevented throughout the operation. In order to design the capstans successfully, we derived and evaluated the kinematics of the proposed exoskeleton glove, which are described in Section IV.

In the proposed design, rotational torques are generated in each finger joint as a result of linear pulling forces that are directed towards the palm. This may be an issue in some cases, since the cables might generate pressing forces in the palm direction instead of finger flexion/extension torques. However, if the glove is snugly fitted on the hand and the tendons are controlled without mutual interference, this issue can be minimized. The wearers did not report any discomfort due to this issue during the experiments, and therefore we did not investigate this matter in our research.

The only components of the proposed exoskeleton glove which are placed remotely from the hand are the control unit and the battery, with their respective electronic circuits. This configuration allows the developed device to be highly portable.

### B. Key Features of the Glove

The developed glove has the following key features:

**Bidirectional action**: The proposed exoskeleton glove supports both finger flexion and extension motions for a thumb and 3 fingers, leaving out the little finger. Each finger is controlled independently and is driven by a pair of cables, one of which is responsible for flexion and the other one for extension. In such a configuration, the cables act in a fashion similar to human tendons and force each finger to move in the desired direction when the cable is being pulled by the motor. This design allowed us to use only 4 actuators, which were installed directly on the dorsal side of the palm. This approach helped to overcome the first challenge for the devices for hand support devices described above, namely, the limited space.

**Wearability**: To make the system light and compact, we chose a soft structure as the framework of the glove. In addition, efficient transmission allows the use of miniaturized motors to provide the required power, which also positively contributes to the light weight of the overall device. To minimize lateral deformations of such a soft exoskeleton and maintain accurate control, we designed an additional lightweight plate and installed it inside the glove to give the framework around the palm more support. Lastly, an effective cable routing architecture helps to minimize undesired palm squeeze. As a result, compact size and low weight of the device make it portable and wearable, while the rigid plate helps to maintain high positioning accuracy of the fingers. This approach helped to address the second challenge, a trade-off between accuracy of the device and its weight and compactness. For more details on the rigid plate and cable routing, the reader is referred to subsection III-D.

**High power-to-weight ratio**: Achieving this feature required implementation of light yet powerful actuators and minimizing power losses in the transmission mechanism. Electric DC motors were chosen as actuators, as they are compact and simple in maintenance. To improve the efficiency of the mechanical transmission between the motors and the fingers, we decided to install the actuators directly on the dorsal side of the hand and to transfer the force by low-friction cables made of a composite material (Dyneema), without the use of any intermediary mechanisms, such as Bowden cables. With this design, the actuators are easy to maintain, and the device is mechanically simple, quiet and does not suffer from misalignments of the tendons. As a result, we were able to address the third challenge, namely, implementation of efficient and easy-to-maintain actuators. More details on the actuator placement are presented in subsection III-C.

**Free wrist**: Installing the motors directly on the hand preserves full mobility of the other joints of the arm, such as the wrist. Therefore, they can be either left free during the operation of the glove or assisted independently by another devices, if needed.

**Comfort**: The overall soft structure of the glove and adjustable Velcro straps around the fingers allow easy donning and doffing, as well as adjustment, of the system on hand of different sizes and shapes.

The following subsections describe each of the mentioned features in more details.

### C. Actuator Placement

To actuate the tendons in the proposed glove, the motors can be placed either on the palm itself or installed remotely (e.g., at the forearm), as shown in Fig. 3, right. Direct placement of the motors increases the weight of the wearable part of the system. At the same time, it allows smaller, less powerful motors to be used to generate the desired grasping force because power losses in transmission are decreased, which helps to reduce the size and weight of the overall system. Alternatively, the motors can be placed remotely from the hand; however, this requires some type of mechanism to transfer the motor energy to the fingers.

One of the most straightforward and lightweight solutions to remote actuator placement is to use Bowden cables, although this approach may introduce a number of issues, including the addition of a large amount of nonlinear friction into the system. A number of research works have been dedicated to characterizing Bowden cable friction as a function of cable speed, materials with different friction coefficients, and deflection angle [20]. It is common to estimate the friction inside a Bowden cable by the so-called capstan equation: $F = e^{\mu\theta}$, where $\mu$ is the friction coefficient between the Bowden cable's sheath and the tendon passing through it, and $\theta$ is the deflection angle of the Bowden cable. We assume that, during wrist flexion or hyper-extension, the value of the wrist angle (and therefore the Bowden cable deflection angle $\theta$) may reach up to 90 degrees; and that the friction coefficient $\mu$ between the tendons and the Bowden cable is 0.2. The capstan equation suggests that in this case, the force required from the actuator to flex the fingers should be at least 36.9% higher than when the actuators are placed directly on the palm. In order to keep the same output while using remote actuator placement, this design would require a gearbox with a higher reduction ratio in terms of hardware. However, higher motor power requirements may not always be satisfied simply by increasing the gear ratio, since higher-rated gears would be heavier and also slower, both of which are undesirable.

Either one of the approaches described above (direct or remote actuator placement) can be employed in the design of the glove. However, since we originally considered the compactness and low weight of the system to be our main design priorities, we opted for direct motor placement.

A conceptual drawing of the developed glove is presented in Fig. 4. A module with 4 actuators is placed on the back (dorsal) side of the hand to improve transmission efficiency. At the same time, this placement of actuators required an optimized cable routing system. This feature is discussed in the following subsection.

### D. Cable Routing

The compliant human muscles and stiff tendons of a healthy hand can position the fingers with a high degree of accuracy. In a human hand, the tendons travel along the fingers' bones, while being protected from undesired stretching by sheaths attached to the bones near the joints (Fig. 4). To emulate this structure, we designed the glove with the following features: A single cable was used for flexion or extension, and it was guided along the central axis of the finger. This approach decreases friction and therefore improves transmission efficiency. If the mentioned cable is properly aligned, it should not generate any undesired abduction or circumduction finger motions. However, two cables can be used for a more stable extension motion. Next, adjustable Velcro straps were used to attach the tendons and cable guides to the finger and to prevent possible stretching of the glove material which the pulleys are mounted on. In this case, the Velcro straps play the role of human skin, holding the soft structure together. A set of cable guides, acting in a fashion similar to the tendon sheaths of the human hand, were placed along the phalanges. The locations of the guides are similar to the corresponding sheaths. The carpal sheath of the human hand, denoted by $S_c$ in Fig. 4 surrounds the finger flexor tendons, thus preventing their lateral displacement during wrist flexion. We assumed that the distance between the carpal and metacarpal ($S_m$) sheaths remains constant during hand flexion and extension. Under this assumption, the locations of the sheaths beginning with the metacarpal sheath $S_m$ and ending with the distal sheath $S_d$, are crucial to achieve anatomically correct and powerful grasping. Therefore, in our glove design, it was only necessary to mimic the aforementioned natural sheaths, and their glove counterparts are labeled by $P_m$ (metacarpals), $P_p$ (proximal phalanx), $P_i$ (intermediate phalanx), and $P_d$ (distal phalanx) in Fig. 4.

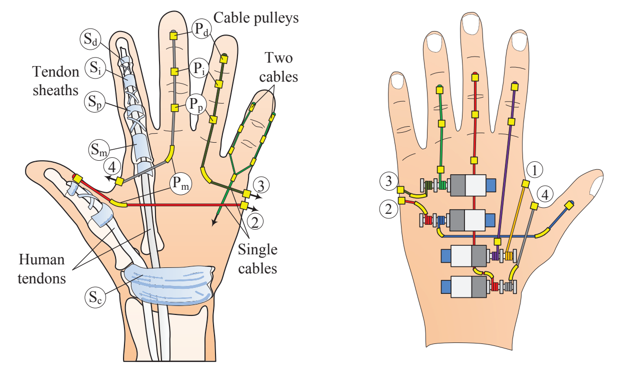


Fig. 4. Cable routing VS hand structure (left); A schematic drawing of actuators placed on a dorsal side of the hand and their respective cables (right);

There are several cable-driven exoskeleton gloves with a similar actuation concept [8]-[10], [16]. However, the main difference and challenge of our cable-driven actuation mechanism originated with the fact that the cables needed to be routed from actuators installed on the dorsal side of the hand, and therefore they travel to the palmar side around both sides of the hand. Despite providing certain advantages, this approach may also cause problems when the palm is laterally squeezed by the cables under high tension. More details on this issue and its solution are presented in the following subsection. We did not specifically investigate the transmission efficiency of the selected cable routing map, however, the analysis of experimental data of grasping and pinching forces suggested that it was on the order of $60 - 70\%$.

This article has been accepted for publication in a future issue of this journal, but has not been fully edited. Content may change prior to final publication. Citation information: DOI 10.1109/TMECH.2016.2641932, IEEE/ASME Transactions on Mechatronics



### E. Removing Hand Squeeze

The placement of actuators on the dorsal side of the hand and the need to leave the palm free requires the flexor cables to be routed from the dorsal to the palmar side of the hand. Since the glove itself is soft, an increase in the tension of the flexor cables may result in deformation of the glove and 'squeezing' of the palm inside it. This hand squeeze may cause severe discomfort to the wearer during operation. In addition, hand squeeze negatively affects positioning accuracy and the maximum grasping force of the glove, since in this case, the energy provided by the actuators is partially used to deform the glove with the hand inside, instead of flexing the fingers.

This issue was solved by introducing a light rigid plate which repeated the anatomical shape of the hand, as shown in Fig. 3 (right). The plate is made of a medical fiberglass cast tape and is installed directly inside the glove. Due to the high stiffness of the material, the plate prevents the lateral squeeze of the soft glove and does not cause any discomfort to the wearer. As a result, the force generated by the actuators can be more effectively transferred to the fingers and induce their flexion and extension instead of the undesired palm squeeze. The palmar side is only partially covered by the plate, which provides greater freedom of motion and leaves the palm free for object grasping.

## IV. Glove Kinematics

The kinematic model of the finger is derived in this section to estimate the amount of tendon contraction required for finger flexion and extension, i.e. how much of the tendon cable needs to be wrapped around the motor's capstan so that the finger flexes completely and then extends to its initial position. The contractions required by the flexor and extensor tendons may differ significantly from each other because of differences in the cable routing and in the relative motion of the cable guides with respect to the finger joints. Knowing the maximum values of the flexor and extensor tendons' contractions allows the design of asymmetrical motor capstans which consist of two cylinders of different diameters and can therefore compensate for the difference in flexor and extensor kinematics. This design enables bidirectional actuation of the thumb and each finger without cable slacks, while using only a single motor per finger. In addition, the developed kinematics model of the glove can be used for force analysis and design of the optimal placement of cable guides on the fingers.

To derive the kinematic model of the proposed exoskeleton glove system, we considered each human finger to be acting as a serial manipulator consisting of a base (metacarpals) and three links corresponding to finger's phalanges, as shown in Fig. 5a). The phalanges are: proximal ($\mathbf{O}_0$-$\mathbf{O}_1$), intermediate ($\mathbf{O}_1$-$\mathbf{O}_2$), and distal ($\mathbf{O}_2$-$\mathbf{O}_3$), and the matrices $\mathbf{O}_i$ are $4 \times 4$ homogeneous transformation matrices denoting the orientation and position of each joint. Matrices $\mathbf{F}_i$ and $\mathbf{B}_i$ are also $4 \times 4$ homogeneous transformation matrices denoting the position and the orientation of the guides which the tendons pass through on the front (flexor tendon) and back (extensor tendon) side of the hand, respectively. It should be noted that the total number of back-side guides is one less than the number

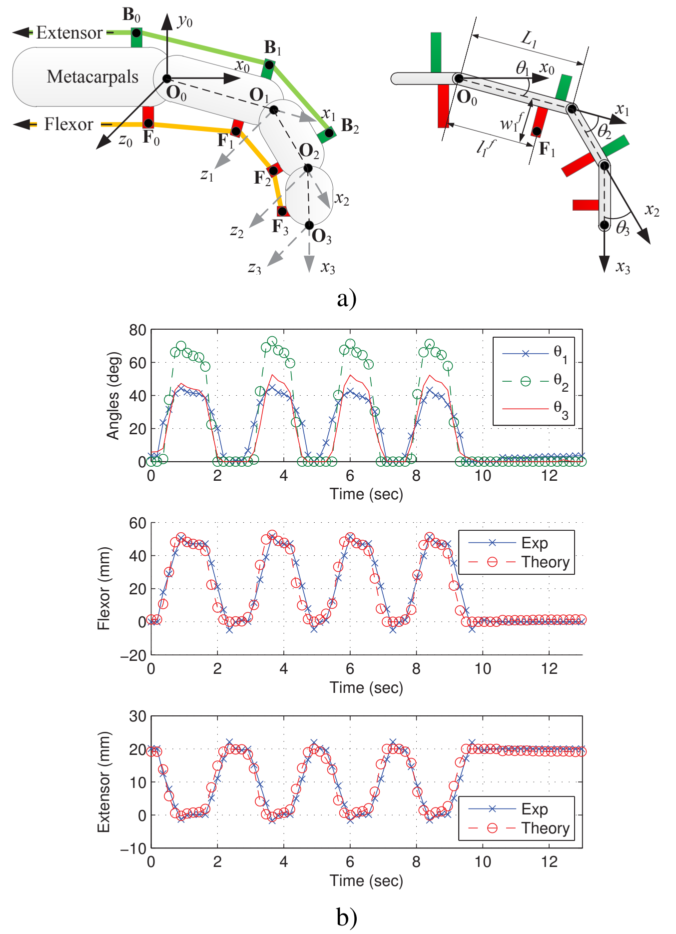


Fig. 5. a) A schematic finger diagram for kinematics evaluation; b) Index finger kinematics during free flexion. Proximal ($\theta_1$), intermediate ($\theta_2$), and distal ($\theta_3$) phalanges' angles (top); experimental and theoretical contractions of the flexor (middle) and extensor tendons (bottom)

of front-side guides because, during the human studies, the subjects reported that they experienced an uncomfortable feeling during the extension motion when a third guide $\mathbf{B}_3$ was attached at the dorsal side of the distal joint. We believe this was due to the fact that the tendons responsible for finger extension in the human hand, namely extensor indicis and extensor digitorum muscles tendons, have an insertion point in the middle phalanx of the fingers. Thus, an unconstrained human finger is naturally not capable of extending the distal phalanx independently of the intermediate one. This comes in contrast to the flexing tendons (for instance, flexor digitorum profundus) of the hand, which have an insertion point at the base of distal phalanges of the fingers. When designing the glove, we wanted to replicate the natural structure of the hand as closely as possible, and decided to place the insertion point of the motor tendons of the proposed glove at the intermediate phalanx, just like it happens in the human hand.

The coordinates of any point of a serial manipulator can be found using the Denavit-Hartenberg convention. With the selected structure, each phalanx will only have 2 non-zero DH parameters, namely, link length $L_i$ and joint angle $\theta_i$, with $i = 1, 2, 3$ corresponding to the proximal, intermediate, and distal phalanges, respectively.

The guides $\mathbf{F}_0$ and $\mathbf{B}_0$ are rigidly attached at the metacarpal phalanges of the hand and are considered immobilized in the kinematic model. The global coordinates of the tendon guides $\mathbf{F}_i$ and $\mathbf{B}_i$ depend on joint angle $\theta_i$ and the guide's placement relative to respective joint $\mathbf{O}_{i-1}$. The length of phalanx $i$ along axis $x_i$ is denoted by $L_i$. For the front-side guides, the relative position of each guide $\mathbf{F}_i$ measured from the origin $\mathbf{O}_{i-1}$ to the guide with respect to the $x_i$-axis is denoted by $l_i^f$, while the offset along the $y_i$ axis is denoted by $w_i^f$. Parameters $l_2^f$, $l_3^f$, $w_2^f$, and $w_3^f$ are not shown in Fig. 5(a) or the sake of simplicity. The same notation can be applied to the extensor guides located on the dorsal side of the palm and fingers $\mathbf{B}_i$.

The homogeneous transformation matrices for each joint are as follows:

$$\mathbf{O}_i = \begin{bmatrix} RO_i^0 & o_i^0 \\ 0 & 1 \end{bmatrix} \qquad (1)$$

where $\{i \in \mathbb{Z} : 1 \leq i \leq 3\}$ is the joint's index, $RO_i^j \in \mathbb{R}^{3\times3}$ are the matrices denoting the orientation of frame $i$ with respect to frame $j$, while the terms $o_i^j \in \mathbb{R}^{3\times1}$ are vectors denoting the position of frame $i$ relative to frame $j$.

Using this notation, one can write

$$\mathbf{F}_i = \begin{bmatrix} RF_i^0 & f_i^0 \\ 0 & 1 \end{bmatrix} \qquad (2)$$

where $RF_i^0$ is orientation and $f_i^0$ is position of flexor guide $\mathbf{F}_i$ with respect to the origin $\mathbf{O}_0$. One can find position of each of the front flexor guides $f_i^0$ to be

$$f_i^0 = o_{i-1}^0 + l_i^f \begin{bmatrix} \cos\theta_{1..i} \\ \sin\theta_{1..i} \\ 0 \end{bmatrix} + w_i^f \begin{bmatrix} -\sin\theta_{1..i} \\ \cos\theta_{1..i} \\ 0 \end{bmatrix} \qquad (3)$$

where $i$ is the index of the $i$-th flexor guide and the angles are $\theta_{1..1} = \theta_1, \theta_{1..2} = \theta_1 + \theta_2, \theta_{1..3} = \theta_1 + \theta_2 + \theta_3$. Positions of the extensor tendons $b_1^0$ and $b_2^2$ can be found accordingly through respective positions of 2 extensor guides $\mathbf{B}_1$ and $\mathbf{B}_2$.

The kinematics of the flexor and extensor tendons can be significantly different, as the offsets $w_i^f, w_i^b$ and positions $l_i^f, l_i^b$ of each pair of the palmar and dorsal cable guides $\mathbf{F}_i$-$\mathbf{B}_i$ differ significantly from each other.

With the accepted notation, the length of the flexor tendon between the guides $\mathbf{F}_0$ and $\mathbf{F}_3$ can be found as

$$X^f = \|f_1^0 - f_0\| + \|f_2^0 - f_1^0\| + \|f_3^0 - f_2^0\| \qquad (4)$$

where $f_0 = \begin{bmatrix} l_0^f & w_0^f & 0 \end{bmatrix}^T$ is the position of guide $\mathbf{F}_0$ with respect to $\mathbf{O}_0$. As for the extensor tendon, its length between points $\mathbf{B}_0$ and $\mathbf{B}_2$ is

$$X^b = \|b_1^0 - b_0\| + \|b_2^0 - b_1^0\| \qquad (5)$$

where $b_0 = \begin{bmatrix} l_0^b & w_0^b & 0 \end{bmatrix}^T$ is the position of guide $\mathbf{B}_0$ with respect to the origin $\mathbf{O}_0$. Two final equations (4) and (5) represent the inverse kinematics problem of the glove.

The flexor tendon will reach its maximal length $X_{max}$ when the finger is fully extended ($\theta_{1,2,3} = 0$). Therefore, the linear tendon contraction $\Delta X$ can be found for the known as

$$\Delta X^f = X_{max}^f - X^f \qquad (6)$$

Likewise, one can derive the equation for the extensor tendon, which will reach its maximum length $X_{max}^b$ when the finger is fully flexed.

The proposed kinematic model was experimentally verified in a series of free palm flexion and extension tests. During the experiments, the palm was repeatedly flexed and extended by the exoskeleton, and the joint angles were recorded. The experimental tendon contraction was calculated to be $\theta_m \cdot r$, where the terms $\theta_m$ and $r$ denote motor angle and the radius of the capstan, respectively. The theoretical contraction of each tendon was calculated as follows: measured angle values $\theta_1, \theta_2, \theta_3$ were subsequently substituted into Eq. (3), and the forward kinematics problem of the glove (4)-(5) was solved to find the values of tendon contraction corresponding to a given set of finger joint angles. If the proposed kinematic model did not describe the system accurately, experimental and theoretical values of tendon contraction would not match each other.

The experimental results of index finger flexion and extension are presented in Fig. 5b). A high correlation between the theoretical and experimental curves was observed during the experiments, with the values of root-mean-square (RMS) errors being 5.85 mm for the flexor tendon and 2.13 mm for the extensor tendon, respectively, which constituted an error of approximately 9%. We consider these results satisfactory for our design, since the device operated in the presence of friction between the cables and the guides and kinematic uncertainties introduced by the soft structure of the glove. As a result of experimental verification of the model, we determined the diameters of the motor capstans for wrapping flexor and extensor cables to be 12.5 mm and 5 mm, respectively, thus maintaining the 5:2 ratio suggested by Fig. 5b).

## V. Evaluation of Glove Performance

### A. Glove Prototype

A prototype of the glove was composed of three layers (Fig. 6 (a)) which included an elastic glove, adjustable Velcros, a rigid plate and the exoskeleton itself (motors, tendons, and guides). Four 1.5-Watt Maxon motors (A-max 19), each equipped with a 32 CPT encoder and a gear with a 84:1 reduction ratio, were used as actuators. The artificial tendons were Dyneema lines with a diameter of 0.6 mm. All other parts (motors mounts, frame, motor pulleys, tendon guides) were 3-D printed. Velcro stripes were used to tighten the base-plate around the hand and to attach tendon guides at the phalanges. Therefore the device is also adjustable for various hand sizes. The angles between the phalanges were measured using resistive flex sensors (SpectraSymbol SEN-10264, length 5.5 cm). The overall weight of the wearable prototype glove is 250 g. The glove is driven by a control unit which includes an Arduino Uno microcontroller board coupled with an Adafruit motor shield that is capable of controlling up to 4 DC motors simultaneously. The device is powered by a conventional 11.1-V Li-Po battery. Accordingly, the developed prototype is completely untethered from any control station. A fully mobile version of the glove is shown in Figure 6 (a).

To initialize a grasping motion, we installed an infrared distance sensor at the palmar side of the wrist (Fig. 6 (b))

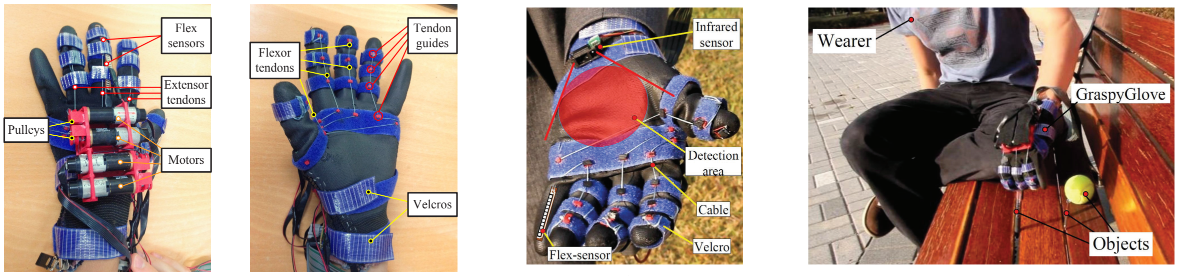


a) b) c)

Fig. 6. Graspy Glove: a) Overview of the portable version b) Integration of infrared and flex sensors c) Appearance during outdoor tests

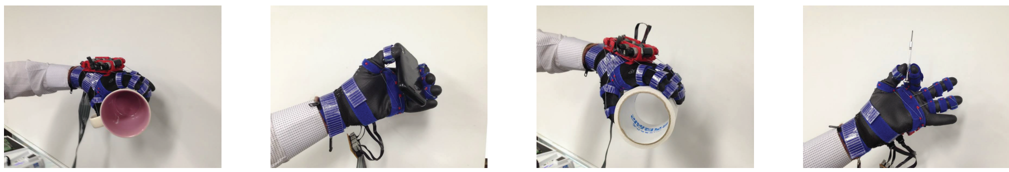

a) b) c) d)

Fig. 7. Versatile object grasping: a) cup, b) smartphone, c) paper roll, and d) screwdriver

and attached an additional flex sensor at the little finger inside the glove. Automatic and manual activation algorithms were implemented to allow the wearer to grasp the objects. Since the motion of the little finger is not restricted by tendons, the wearer can freely flex and extend it at any given time, which can be interpreted as the wearer's intention to open or flex the hand. Thus, in manual control mode, the wearer could initiate and stop grasping by simply flexing the little finger. Likewise, the operator could give the command to open the palm by bending the little finger in the opposite direction.

In the automatic control mode, when the human reaches out to grasp an object, the object comes into the proximity of the infrared sensor which detects the object and triggers the motors to start grasping. The grasping motion is completed when the object exerts enough force to press any of the push buttons installed at the tip of every finger and the thumb.

### B. Glove Usability Test

To check the usability of the developed exoskeleton glove, called GraspyGlove, it was first tested in a series of indoor object grasping experiments. The wearer was able to successfully grab and hold rigid objects such as a 300-g china cup (Fig. 7(a)) and a smartphone (Fig. 7(b)). It was also possible to grab a paper roll (Fig. 7(c) with a diameter of 90 mm with the help of the GraspyGlove. In addition, the human subjects could perform a precise pinching grasp to hold miniature objects, such as the screw driver in Fig. 7(d) with a diameter of 3 mm. GraspyGlove could execute both a precision grip and power grip, and therefore can be used to cover a large range of the prehensile activities of human hand.

Fig. 8 presents a sample pattern of the index finger joint angles observed during the object grasping tests. In this experiment, the proximal phalanx ($\theta_1$) was initially blocked by the object (a stiff rubber ball), as shown in Fig. 8 (a). Therefore, after the motion starts at approximately 0.4 sec, whole flexor contraction is directed exclusively into actuation of the intermediate and distal phalanges (the left-most dashed line in the graphs in Fig. 8). After the finger completely envelops the object at the time instance of around 0.7 sec (the middle dashed line on the graphs corresponding to the case (b) on the diagram below), the phalanges cannot flex freely anymore because of high object's stiffness. However, since the motor is still contracting the flexor, the tension force acting on the cable increases, which results in the motion of the proximal phalanx that deforms the object (this period of time marked as (c) on both the graphs and kinematical structure at the bottom) and compression of the soft parts of the glove. This motion starts at 0.7 sec and finishes at approximately 1 sec. During this period of time, a certain deviation between the experimental and theoretical curves can be observed. Theoretical curve only reflects the displacement of the cable caused by the motion of finger joints (angles $\theta_1 - \theta_3$). Since after 0.7 sec all phalanges are already in contact with the object, all of their displacement contributes to the deformation of mentioned object. For clarity, the region corresponding to object deformation is filled with red color in the flexor contraction plot in Fig. 8. At the same time, a certain part of excessive tendon tension contributes to stretching of the soft parts of the glove (the Velcros and elastic material), and because of this the actual contraction of the cable is larger than the one calculated from current joint angles. This motion region is filled with blue color in Fig. 8. If needed, the issue of undesired stretching of the glove will be addressed in the future versions of the device. However, in the current state of the glove, the error between theoretical and actual tendon contraction curves can be used by the control system as an indicator of external disturbance (e.g. an object). These experiments demonstrated that the glove could generate sufficient grip force when grasping objects. Prevention of excessive grasping forces can be solved at the control level. For instance, the flexion can be stopped once a

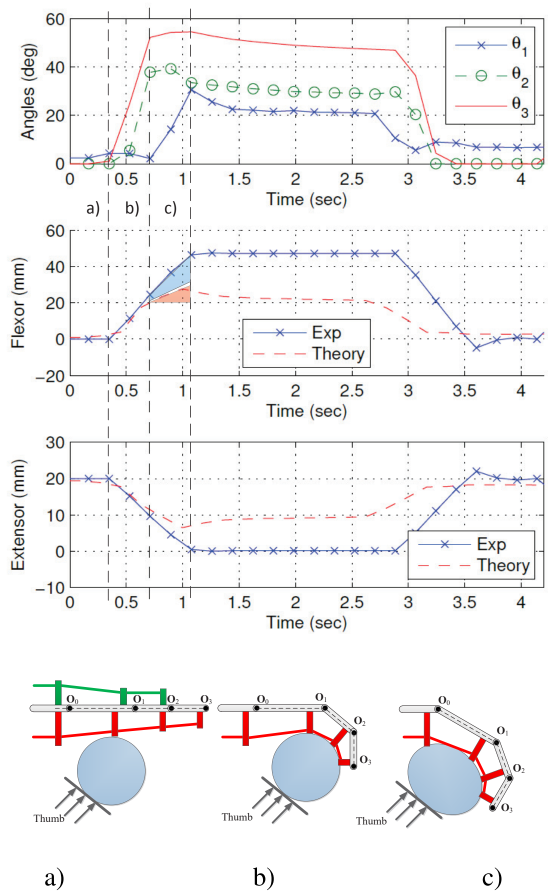


Fig. 8. Wrap of index finger around an object: Proximal ($\theta_1$), intermediate ($\theta_2$), and distal ($\theta_3$) phalanges' angles (top); experimental and theoretical contractions of the flexor (second row) and extensor tendons (third row). Finger configurations (bottom row, left to right): $t$=0 s, $t$=0.7 s, $t$=1.0 s

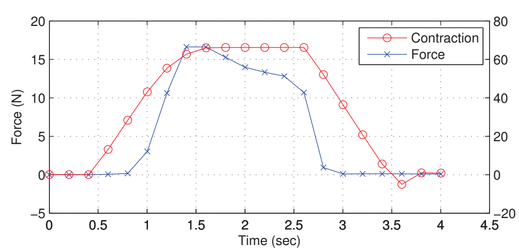


Fig. 9. Grasping force generated by pinch motion

certain value of motor torque is reached or if some triggering mechanism (e.g., force sensors at the fingertips) is activated.

In addition, since the glove is portable and untethered, we were able to perform a series of similar object grasping and handling tests outdoors. A snapshot of the wearer during these tests is shown in Fig. 6 c). The experiments demonstrated that a 3000-mAh battery used to power the device allowed the glove to perform continuous flexion and extension of the palm for up to 4 hours. A video featuring performance of the proposed glove is available online[1].

[1]https://www.youtube.com/watch?v=BaCVT3BNppE

### C. Force Measurement

The force generated by the pinching motion of the glove was measured when each finger was flexed toward the thumb. An ATI NANO 6-DOF force sensor (ATI Industrial Automation) was used in the experiments. The sensor was placed between the thumb and each finger. The fingers and the thumb were subsequently actuated, and the resulting force was recorded. To eliminate any human influence on the experimental results, the glove was placed around a dummy 3D-printed hand having realistic human hand dimensions and degrees of freedom.

A typical pattern of tendon contraction and generated pinch force for the index finger is presented in Fig. 9. It can be observed that the maximum force generated by the pinch motion is approximately 16 N. In addition, one can notice that the force value gradually drops down to approximately 11 N, even though the motors remain still. This effect is caused by the soft structure of the exoskeleton and the existence of friction between the tendons and the guides. The forces acting at the finger joints require a certain amount of time to redistribute themselves after grasping, even if the cable is immobilized. We plan to address this force drift issue in a future version of the device.

During the force experiments, the force sensor was gripped between the index finger and the thumb and the motors were stalled. The motors implemented in the glove could generate the maximum continuous torque of 3.51 mNm. When coupled with the 84:1 gearhead and pulleys of the 5 mm radius, a pair of antagonistically placed actuators could generate the maximum linear (pulling) force of approximately 45 N, taking into account efficiency of motor and gear (70% and 73%, respectively). Since the forces generated normal to the fingertip are determined by the configuration of the fingers and the moment arms of the cable, the force applied to the sensor will always be smaller then a (pulling) force of the cable. The combination of guides and kinematics of the hand introduces a reducing transmission. The force can be improved by increasing the offset of the guides, although this may negatively affect grasping abilities of the glove.

## VI. Comparison of Existing Systems for Hand Assistance and Rehabilitation

A summary of the exoskeleton gloves for hand rehabilitation and assistance developed in the recent decade is presented in Table I, and a comparison chart of these devices is shown in Fig. 10. The six axes in each plot are the 6 features of the devices summarized in Table I (overall weight of the system, the weight of the wearable part only, pinch force, number of fingers being assisted, free wrist, bidirectionality), with their values scaled from 20 (corresponding to the inner hexagon area of the grid) to 100 points. Two of the axes, namely 'Bidirectional', and 'Free wrist', are binary, and their values are either 20 (false) or 100 (true). The developers of RoboGlove [18] did not provide information on pinch force and mentioned only the value of a power grasp force (89 N). Since in our evaluation we aimed to compare the pinch forces generated between the thumb and index fingers, we decided to take a reference value of 40 N for the pinch force of the

This article has been accepted for publication in a future issue of this journal, but has not been fully edited. Content may change prior to final publication. Citation information: DOI 10.1109/TMECH.2016.2641932, IEEE/ASME Transactions on Mechatronics



TABLE I
CHARACTERISTICS OF WEARABLE HAND-ASSISTANCE SYSTEMS

| Device | Actuators | Weight: glove / total | Peak pinch force | Fingers | Free wrist | Bidirect. | Score |
|---|---|---|---|---|---|---|---|
| Ryu et al. [12] | hydraulics, cables | 2.62 kg / 2.74 kg | 12 N | 3 | ∨ | - | 44% |
| Nycz et al. [16] | linear motors, cables | 113 g / 867 g | 8.7 N | 4 | ∨ | ∨ | 78.1% |
| Gloreha Lite [14] | motors, cables | 80 g / 5 kg | 5 N | 5 | ∨ | ∨ | 73.7% |
| Hand of Hope [13] | linear motors, links | 700 g / n/a | 12 N | 5 | ∨ | ∨ | 68.9% |
| SNU Exo-Glove [9] | DC motors, cables | 194 g / n/a | 20 N | 3 | ∨ | ∨ | 70.4% |
| NASA RoboGlove [18] | DC servomotors, cables | n/a / 770 g | 40 N (estimated) | 5 | ∨ | - | 68.8% |
| **Graspy Glove (this paper)** | **DC motors, cables** | **250 g / 340 g** | **16 N** | **4** | ∨ | ∨ | **80.2%** |

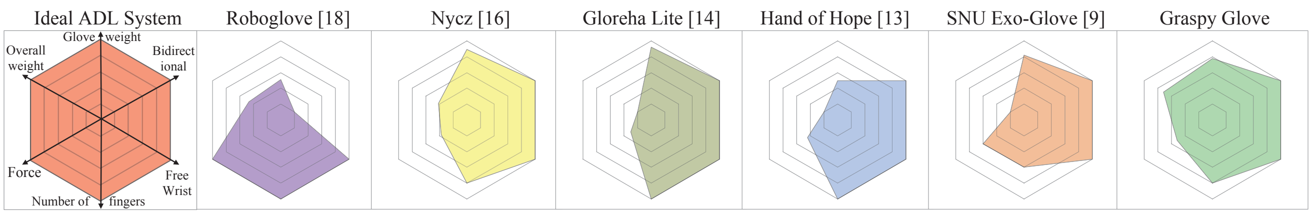


Fig. 10. Comparison chart of existing gloves for rehabilitation and assistance

RoboGlove to compare it to the rest of the systems correctly. The forces were scaled linearly between 20 and 100, with 100 points corresponding to 40 N. The total weight of the device and the weight of the wearable part were scored separately. The ‘Weight’ axes were inverted so that the maximum weight corresponded to the value of 20, and zero weight to 100 points. The scores were scaled non-linearly according to the formula W = $100/e^x$, with $x$ denoting weight, to better reflect the differences between the weights closer to zero. If the information on the total weight was not available, the device was given a minimum evaluation score of 20 points. If, on the other hand, only the total weight was reported, both weights were considered equal. Finally, the X-glove [15] and the device by Moromugi et al. [8] were omitted from this comparison, as very limited numerical data is available on these devices. Assuming the hexagon area of an ideal system to be 100%, the relative scores of each glove are presented in Table I.

## VII. CONCLUSION AND FUTURE WORKS

This paper proposes a portable hand assistant system for ADL support. We developed a soft and wearable exoskeleton glove and experimentally proved its usability by versatile object grasping while achieving high pinching forces. One of the biggest advantages of the proposed exoskeleton glove is its power-to-weight ratio, which is the highest among existing portable systems for hand assistance. At the same time, the glove can support the flexion and extension of 4 fingers (excluding the little finger) while enabling the wrist to move freely. The use of a cable-driven soft structure, the direct placement of actuators on the back (dorsal) side of the hand, and the optimal cable routing which mimicked real human hand anatomy allowed the development of a compact, bidirectional, and powerful exoskeleton glove. Direct actuator placement allowed us to eliminate any additional friction originating from transmission mechanism. As a result, the designed glove is compact and light and provides the maximum pinch force of 16 N. The resulting weight of the wearable part is as little as 250 g, which includes the weight of 4 actuators, while the total weight of the system is 340 g.

Undesired motor tilting was mitigated by optimized cable routing and motor vibration during the operation was minimal due to the absence of any unbalanced elements as well as certain level of damping was present in the motor mount.

The performance of the glove was experimentally verified in a series of versatile object grasping tests, where the task was to pick up and hold objects of various sizes, shapes, and hardness. The wearers could successfully grasp objects weighing 300 grams and with diameters of up to 90 mm as well as miniature objects. When powered by a conventional 3000-mAh battery, the glove could operate continuously performing grasping task for 4 hours.

To date, we have conducted experiments with 4 healthy subjects, with the tests including versatile objects grasping, measurement of applied force, estimation of range of motion, and others. Most recently, we have started to work with hemiparetic stroke patients, gathering the feedback from the therapists and developing control algorithms. However, we have conducted only one training session, which included basic pick-and-place tasks. The obtained results are too preliminary and therefore are not reported in the manuscript. Additionally, according to feedback we obtained from occupational therapists, GraspyGlove is feasible to assist patients with hand impairment in ADL tasks, such as spinal cord injury patients with C6 and C7 injuries. In that case, the glove can perform the functions of the tenodesis orthosis. We are looking forward to extensive patient trials and evaluation of the proposed system with involvement of some patient groups in the near future.

One of the drawbacks of the originally designed exoskeleton glove was the soft corset of the glove, which allowed for some of the cables to squeeze the operator’s palm and

This article has been accepted for publication in a future issue of this journal, but has not been fully edited. Content may change prior to final publication. Citation information: DOI 10.1109/TMECH.2016.2641932, IEEE/ASME Transactions on Mechatronics



negatively affected positioning accuracy and the maximum grasping force. This issue was solved by introducing a rigid plate which repeated the anatomic shape of the hand and was embedded into the glove. As a result, the force generated by the actuators could be more effectively transferred to the fingertips to produce finger flexion and extension.

Another potential drawback of the proposed system could be undesired finger motions (unnatural grasping sequence, internal rotation, abduction, etc.) induced by the tendons, due to absence of a rigid structure. However, placing the tendon sheaths in accordance with anatomy of the human hand allows for natural finger movement during free grasp and makes it possible to utilize internal rigid structure of the finger bones for operation.

Lastly, the proposed glove only supports the flexion-extension degree of freedom of the fingers and the thumb. However, the latter naturally has a wider range of motion, and its abduction-adduction motion is essential for grasping. In our study, cable guides were specially adjusted for every glove size, so that when the motion is applied, index finger and thumb meet in a desired point to perform a pinch grasp. This approach, however, requires special tuning and may not be applicable for certain groups of patients. In this case, another active DOF (abduction/adduction) should be added for thumb actuation, and we are planning to address this in the future. Additionally, tactile sensors can be mounted at the fingertips to measure contact forces and to ensure safe object grasping.

In addition, this paper proposes a list of requirements and common challenges for hand assistance devices in ADL.

## References


[1] J. Z. Zheng, S. De La Rosa, and A. M. Dollar, "An investigation of grasp type and frequency in daily household and machine shop tasks," in *Robotics and Automation (ICRA), 2011 IEEE International Conference on*. IEEE, 2011, pp. 4169–4175.

[2] C. A. Trombly, *Occupational Therapy for Physical Dysfunction*. Lippincott, Williams and Wilkins, 1989.

[3] S. Rathore, A. Hinn, L. Cooper, H. Tyroler, and W. Rosamond, "Characterization of incident stroke signs and symptoms: findings from the atherosclerosis risk in communities study," in *Stroke, 2002, vol. 33*, 2002, pp. 2718–2721.

[4] G. J. Snoek, M. J. IJzerman, H. J. Hermens, D. Maxwell, and F. Biering-Sorensen, "Survey of the needs of patients with spinal cord injury: impact and priority for improvement in hand function in tetraplegics," *Spinal cord*, vol. 42, no. 9, pp. 526–532, 2004.

[5] E. H. Kim, M. C. Jang, J. P. Seo, S. H. Jang, J. C. Song, and H. M. Jo, "The effect of a hand-stretching device during the management of spasticity in chronic hemiparetic stroke patients," *Annals of rehabilitation medicine*, vol. 37, no. 2, pp. 235–240, 2013.

[6] C.-Y. Yeh, J.-J. J. Chen, and K.-H. Tsai, "Quantifying the effectiveness of the sustained muscle stretching treatments in stroke patients with ankle hypertonia," *Journal of Electromyography and Kinesiology*, vol. 17, no. 4, pp. 453–461, 2007.

[7] S. Ueki, H. Kawasaki, S. Ito, Y. Nishimoto, M. Abe, T. Aoki, Y. Ishigure, T. Ojika, and T. Mouri, "Development of a hand-assist robot with multi-degrees-of-freedom for rehabilitation therapy," *Mechatronics, IEEE/ASME Transactions on*, vol. 17, no. 1, pp. 136–146, Feb 2012.

[8] S. Moromugi, K. Kawakami, K. Nakamura, T. Sakamoto, and T. Ishimatsu, "A tendon-driven glove to restore finger function for disabled," in *ICCAS-SICE, 2009*. IEEE, 2009, pp. 794–797.

[9] H. In, B. Kang, M. Sin, and K.-J. Cho, "Exo-glove: A wearable robot for the hand with a soft tendon routing system," *Robotics Automation Magazine, IEEE*, vol. 22, no. 1, pp. 97–105, March 2015.

[10] F. Vanoglio, A. Luisa, F. Garofali, and C. Mora, "Evaluation of the effectiveness of gloreha (hand rehabilitation glove) on hemiplegic patients. pilot study," in *XIII Congress of Italian Society of Neurorehabilitation, 18-20 April*, 2013.

[11] P. Maciejasz, J. Eschweiler, K. Gerlach-Hahn, A. Jansen-Troy, and S. Leonhardt, "A survey on robotic devices for upper limb rehabilitation," *J. Neuroeng. Rehabil*, vol. 11, no. 3, pp. 10–1186, 2014.

[12] D. Ryu, K.-W. Moon, H. Nam, Y. Lee, C. Chun, S. Kang, and J.-B. Song, "Micro hydraulic system using slim artificial muscles for a wearable haptic glove," in *Intelligent Robots and Systems, 2008. IROS 2008. IEEE/RSJ International Conference on*. IEEE, 2008, pp. 3028–3033.

[13] X. Hu, K. Tong, X. Wei, W. Rong, E. Susanto, and S. Ho, "The effects of post-stroke upper-limb training with an electromyography (emg)-driven hand robot," *Journal of Electromyography and Kinesiology*, vol. 23, no. 5, pp. 1065–1074, 2013.

[14] Gloreha glove. [Online]. Available: http://www.gloreha.com/

[15] K. Triandafilou, J. Ochoa, and D. Kamper, "Effect of static versus cyclical stretch on hand motor control in subacute stroke," *Int J Neurorehabilitation*, vol. 1, no. 124, p. 2, 2014.

[16] C. J. Nycz, T. Bützer, O. Lambercy, J. Arata, G. S. Fischer, and R. Gassert, "Design and characterization of a lightweight and fully portable remote actuation system for use with a hand exoskeleton," *IEEE Robotics and Automation Letters*, vol. 1, no. 2, pp. 976–983, 2016.

[17] V. Parker, D. Wade, and R. L. Hewer, "Loss of arm function after stroke: measurement, frequency, and recovery," *Disability & Rehabilitation*, vol. 8, no. 2, pp. 69–73, 1986.

[18] M. Diftler, C. Ihrke, L. Bridgwater, D. Davis, D. Linn, E. Laske, K. Ensley, and J. Lee, "Roboglove-a robonaut derived multipurpose assistive device," 2014.

[19] D. Carroll, "A quantitative test of upper extremity function," *Journal of chronic diseases*, vol. 18, no. 5, pp. 479–491, 1965.

[20] D. Chen, Y. Yun, and A. D. Deshpande, "Experimental characterization of bowden cable friction," in *Robotics and Automation (ICRA), 2014 IEEE International Conference on*. IEEE, 2014, pp. 5927–5933.


**Dmitry Popov** received his BS and MS degrees in Robotics and Mechatronics from the Moscow State Technical University "STANKIN" in 2009 and 2011, respectively, and his MS and PhD degrees in Mechanical Engineering from Korea University of Technology and Education in 2011 and 2014, respectively. He is currently a Postdoctoral Research Fellow at John A. Paulson School of Engineering and Applied Sciences, Harvard University. His research interests include robotics, human-machine interaction, and novel actuation systems.

**Igor Gaponov** received his BS degree in Automation and Control from the Kursk State Technical University, Russia in 2006, and his MS and PhD degrees in Mechanical Engineering from Korea University of Technology and Education in 2008 and 2011, respectively. He is currently an Assistant Professor at the Department of Mechanical Engineering, Korea University of Technology and Education. His research interests include exoskeletons and assistive devices, human-machine interaction, and nonlinear control.

**Jee-Hwan Ryu** received his BS degree in Mechanical Engineering from Inha University, Rep. of South Korea in 1995, and his MS and PhD degrees in Mechanical Engineering from Korea Advanced Institute of Science and Technology (KAIST), Taejon, Korea, in 1995 and 2002, respectively. He is currently a Professor at the Department of Mechanical Engineering, Korea University of Technology and Education. His research interests include haptics, telerobotics and teleoperation, exoskeletons, and flexible manipulators.